Physics Letters A 394 (2021) 127196

Contents lists available at ScienceDirect

Physics Letters A

www.elsevier.com/locate/pla

Localization properties of a discrete-time 1D quantum walk with generalized exponential correlated disorder

C.V.C. Mendes, G.M.A. Almeida, M.L. Lyra, F.A.B.F. de Moura *

Instituto de Física, Universidade Federal de Alagoas, Maceió AL 57072-970, Brazil

ARTICLE INFO

Article history:
Received 30 December 2020
Received in revised form 26 January 2021
Accepted 27 January 2021
Available online 2 February 2021
Communicated by M.G.A. Paris

Keywords:
Quantum walk
Correlated disorder
Localization

ABSTRACT

We study the dynamics of the 1D Hadamard quantum walk featuring generalized exponential correlated phase disorder. We report the existence of distinct dynamical regimes and discuss the prospect of a judicious tuning of the strength of localization of the walker via the degree of correlation. In particular, we unveil that when the typical correlation length is smaller than the chain size, the maximum spreading of the quantum wavepacket is achieved when the underlying disorder displays Gaussian correlations. Our work provides a framework for investigating the weakening of Anderson localization due to correlated disorder and may also find applications in the context of quantum information processing.

1. Introduction

Anderson localization is one of the most solid concepts in condensed matter physics [1]. It plays a crucial role in metallic-insulator transitions and is the main wave mechanism behind some ubiquitous transport properties displayed by a wide variety of natural and artificial systems. In the simplest scenario, a single particle hopping through a 1D chain featuring a random potential landscape suffers a lack of diffusion thereby remaining trapped around a finite region due to exponential localization of every eigenstate of the system [2].

While the above is true for uncorrelated disorder, it may breakdown in the presence of embedded correlations. First results along this direction came about three decades ago [3,4] addressing the case of short-range spatial correlations. Moreover, the appearance of a band of extended states with sharp mobility edges in 1D systems with long-range correlated disorder was reported in Refs. [5] and [6]. This Anderson-type metal-insulator transition would be experimentally confirmed using waveguides [7] shortly after that. Another interesting class of systems displaying correlated disorder is the one featuring a finite correlation length [8–11]. It has been shown that maximum localization in disordered continuous potentials takes place when the correlation length is of the order of the wavelength [11]. The emergence of extended states as well as the coexistence between disordered and ordered bands are also verified in quasi-1D systems, such as ladder chains [13,14]. For a review of correlated disorder and its impact on Anderson localization phenomena, see Ref. [12].

Many of the disorder configurations discussed above have recently been explored in the light of quantum information processing [15–18]. The motivation is twofold. First, it is desirable to push the limits of such protocols against various forms of noise and, secondly, sometimes disorder can be useful given one is able control it (see, e.g., Ref. [15]). Along this direction, we aim to investigate how correlated disorder affect the dynamics of a discrete-time quantum walk (DTQW) [19,20].

In such, a qubit state (say, on a spin 1/2) is set to propagate by repeatedly applying a unitary operator to a given initial configuration. It first shuffles the internal state of the qubit (more precisely, it generates a superposition) and then shifts its coefficients to the left or right, for a quantum walk on the line, depending on the local spin orientation. By doing it several times, interference effects yield a ballistic spreading profile, in contrast with a diffusive one for the classical random walk, thus providing much faster hitting times. On top of that, DTQWs have been treated as a platform for, e.g., designing quantum algorithms [21], universal quantum computation [22], and studying complex phenomena such as quantum phase transitions [23], topological phases [24–28], localization [24,27,29–36], and even nonlinear phenomena [37–39].

Notwithstanding there are plenty of works addressing the effects of disorder in DTQWs alongside practical implementations [40,41], our goal here is to unveil the subtleties of a transition from strong to weak localization induced by correlated disorder. In a previous work, we dealt with long-range correlations following power law spectrum [36]. Here, in particular, we investigate a class of generalized exponential correlations. These are versatile

* Corresponding author.
E-mail address: fidelis@fis.ufal.br (F.A.B.F. de Moura).

https://doi.org/10.1016/j.physleta.2021.127196
0375-9601/

correlation functions having Gaussian, pure exponential and uncorrelated disorder as particular cases. Furthermore, stretched exponential correlations frequently develops during the relaxation process in glassy materials [42–46]. Exponential correlated disorder models find support on various physical backgrounds. Stretched exponential correlation functions are widely known to arise from the well known Kosterlitz–Thouless-like transition [47]. Similar behavior can also be found for the nematic director field [48], within enzymatic catalytic activity of lipase B from Candida Antarctica [49], in distributions of radio and light emissions from galaxies, and economy, to name a few [50].

In this work we focus on unveiling how the interplay between deviations from Gaussianity and the typical correlation length affects the dynamics of a Hadamard DTQW on the line [20].

2. Model and formalism

The two main ingredients for setting up a DTQW on a 1D array are the coin (qubit) space $\mathcal{H}_C$ spanned by $\{|\uparrow\rangle, |\downarrow\rangle\}$ plus another set $\mathcal{H}_P$ for the position states $\{|n\rangle\}$ $(n = 1, 2, \ldots, N)$, such that the total Hilbert space reads $\mathcal{H} = \mathcal{H}_C \otimes \mathcal{H}_P$ [20]. We now need some operators to act on those states, one of which must carry out the "coin tossing" step. For this, we consider the Hadamard coin,

$$C = \frac{1}{\sqrt{2}} \begin{pmatrix} 1 & 1 \\ 1 & -1 \end{pmatrix}, \tag{1}$$

where it acts solely on the qubit sector $\mathcal{H}_C$. The next procedure is the so-called conditional shift S that moves the walker one way or the other depending on its internal state, that is $S|\uparrow\rangle|n\rangle \longrightarrow |\uparrow\rangle|n+1\rangle$ and $S|\downarrow\rangle|n\rangle \longrightarrow |\downarrow\rangle|n-1\rangle$. Following Ref. [34], we add phase disorder in this very step so that it reads

$$S = |\uparrow\rangle\langle\uparrow| \sum_n (e^{i2\pi\phi_{n+1}}|n+1\rangle\langle n|) + |\downarrow\rangle\langle\downarrow| \sum_n (e^{i2\pi\phi_{n-1}}|n-1\rangle\langle n|), \tag{2}$$

where ϕ_n is some disordered phase. Putting all those elements together, the DTQW is embodied by a unitary operator $U = S(C \otimes I)$ acting on $|\psi(t=0)\rangle$ over and over until in the t-th step $|\psi(t)\rangle = U^t|\psi(t=0)\rangle$.

Let us now make some considerations over the type of disorder we deal with in this work. Instead of assigning a standard (uncorrelated) random box distribution to $\{\phi_n\}$ – as done in [34], where it was shown that localization inevitably sets up for strong enough static disorder – we address a special kind of correlated fluctuations, namely generalized exponential correlated disorder generated from [51]

$$V_n = \sum_{m=1}^{N} \eta_m \exp\left[-(|n-m|/\zeta)^{\alpha}\right], \tag{3}$$

where η_m represents a random phase uniformly distributed in interval $[-0.5, 0.5]$ (independently generated for each sample) and $\{\alpha, \zeta\}$ controls the degree of correlations. The parameter α controls the degree of non-Gaussianity in the disorder distribution. For $\alpha = 0$ there is no disorder. Gaussian correlations correspond to $\alpha = 2$ and the particular case of $\alpha = 1$ accounts for exponentially decaying correlations, where ζ ends up being the standard correlation length [52]. In the limiting case of $\zeta = 0$ one reaches a fully uncorrelated disorder distribution.

We now normalize $\{V_n\}$ such that $\langle V_n\rangle = 0$ and $\langle V_n^2\rangle = 1$, so as to maintain the disorder properties regardless of the system size N, and further define $\phi_n = 0.5\tanh(V_n) + 0.5$ to set its range within interval $[0, 1]$ in order to set the phases in the shift operator [Eq. (2)] in between 0 and 2π. We emphasize that this transformation from V_n to ϕ_n does not affect the correlation profile embedded in the disorder distribution. To have a better look over the resulting phase landscape, in Fig. 1 we show some typical samples of the sequence $\{\phi_n\}$ for various ζ and α values and $N = 10000$. In the same Figure (bottom panels), we plot the corresponding autocorrelation functions, defined as

$$C(r) = \frac{1}{N-r} * \sum_{n=1}^{N-r} \left[(\phi_n\phi_{n+r}) - \langle\phi_n\rangle^2\right], \tag{4}$$

so as to unveil what is going on underneath it. Therein, we clearly see the role of parameters ζ and α. The former acts by smoothing up the fluctuations, what increases the degree of correlations within the disorder distribution. This results in a slower decay of the autocorrelation function with distance r. Now keeping ζ fixed, the behavior of α is much more subtle. It strongly depends on ζ and N in a way it may either hold the decay of the correlation function for longer r or push it more critically (see Fig. 1; compare the outcomes for $\zeta = 1$ and $\zeta = 1000$ in particular). Later on, we will see that this ultimately depends on the ratio ζ/N.

Throughout this paper, our analysis is largely built upon the wavepacket spreading (standard deviation)

$$\sigma(t) = \sqrt{\sum_n (n - \langle n(t)\rangle)^2 P_n(t)}, \tag{5}$$

where $P_n(t) = |\langle\psi(t)|\uparrow, n\rangle|^2 + |\langle\psi(t)|\downarrow, n\rangle|^2$ is the walker's occupation probability at the n-th site and $\langle n(t)\rangle = \sum_n nP_n(t)$ is the average position.

3. Results and discussion

In this section we display and discuss our numerical results for the disordered DTQW featuring generalized exponential correlations introduced previously. The initial state is localized (and symmetric in respect to the coin) in the middle of the chain at $n_0 = N/2$ having the form

$$|\psi(t=0)\rangle = \frac{1}{\sqrt{2}}|\uparrow, n_0\rangle + \frac{i}{\sqrt{2}}|\downarrow, n_0\rangle, \tag{6}$$

for all the simulations below. In addition, every plotted quantity is averaged over 1000 independent realizations of disorder unless stated otherwise. We first show the general profile of the time evolution of the walker in Fig. 2 where we display the space-time diagram for $P_n(t)$ for a representative value of α and correlations length ζ representing short and long-ranged correlated disorder. We clearly observe that for short-ranged correlated disorder ($\zeta = 1$) the walker remains fully localized around its initial position. This should come with no surprise as the underlying correlations are effectively low and disordered DTQWs share some similarities with Anderson localization theory [24,27,29–34]. For long-ranged correlated disorder ($\zeta = 1000$), we spot a significant portion of the probability amplitude coming out of n_0 whereas a finite fraction of the initial packet is still retained around the initial site. This is another characteristic of the localized nature of the quantum walker. Next, we move towards a more accurate description of the localization properties of the system by analyzing $\sigma(t)$ in chains with different sizes.

In Fig. 3 we plot the time evolution of the standard deviation $\sigma(t)$ versus t/N for $N = 2000$ up to 16000. For short-range correlations ($\zeta = 1$) the wavepacket width displays an initial diffusive spreading with $\sigma \propto t^{1/2}$. This indicates that the initial spreading

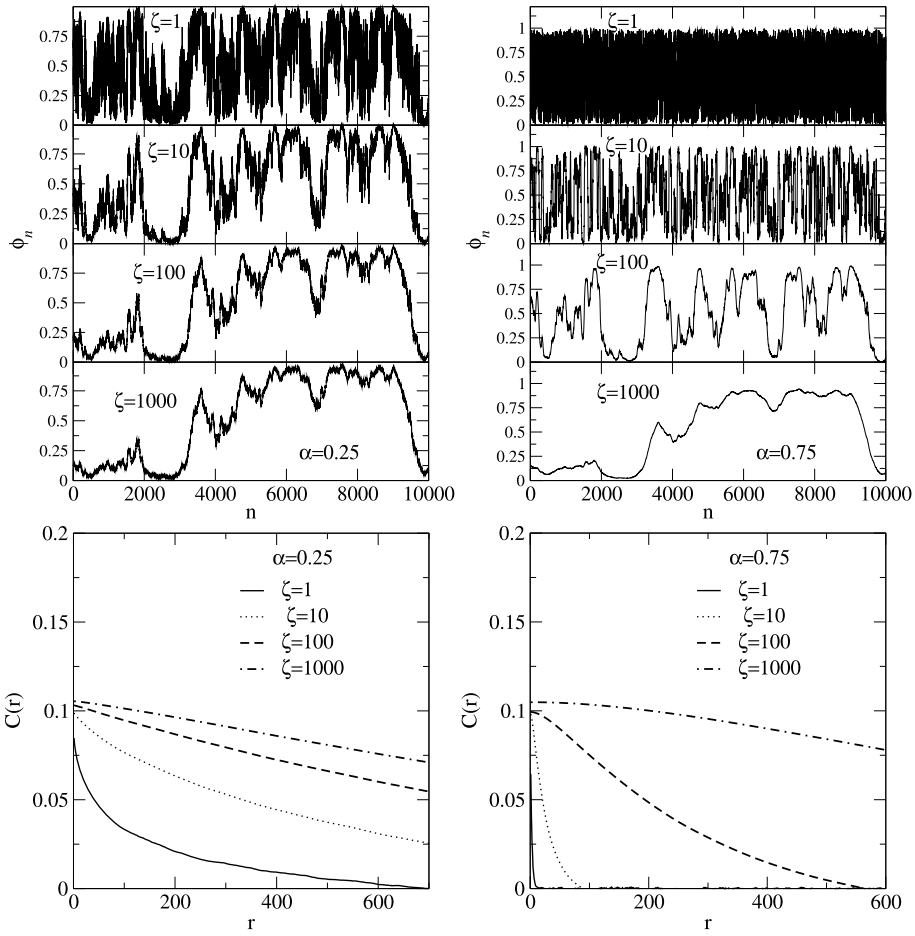

Fig. 1. Top: typical, one sample series of $\{\phi_n\}$ for $\alpha = 0.25, 0.75$ and $\zeta = 1, 10, 100, 1000$ with $N = 10000$. Bottom: corresponding autocorrelation functions generated by $C(r) = [1/(N-r)] * \sum_{n=1}^{N-r} [(\phi_n \phi_{n+r}) - \langle \phi_n \rangle^2]$ averaged over 30 independent samples, against r.

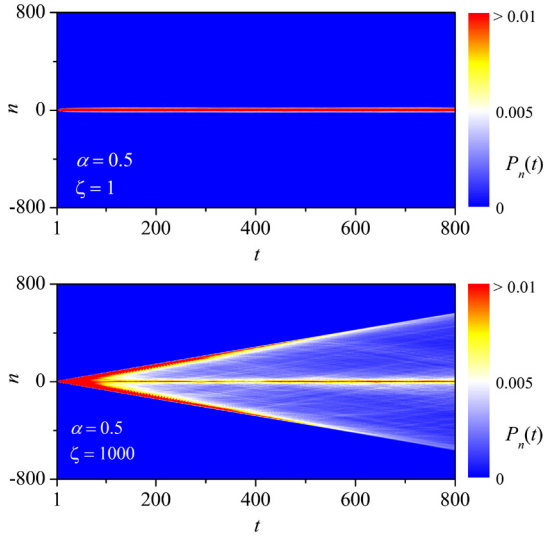

Fig. 2. Time evolution of the occupation probability $P_n(t)$ versus n for $\alpha = 0.5$ and $\zeta = 1$ (top panel) and $\zeta = 1000$ (bottom panel). Notice that the walker remains fully localized for short-ranged correlations while a significant part of it spreads out in the case of long-range correlated disorder. (For interpretation of the colors in the figure(s), the reader is referred to the web version of this article.)

is already strongly influenced by the underlying disorder. At long-times, the wavepacket width saturates at a finite size-independent value signaling Anderson localization. For long-ranged correlated disorder ($\zeta = 500$ and 1000), the initial spreading becomes ballistic, thus not being affected by disorder and becoming similar to the one taking place in a disorder-free DTQW. (In this case, saturation of the wavepacket width at $t \simeq N$ occurs due to finite size effects.) It is clear to spot from Eq. (3) that taking the limit $\zeta \to \infty$ renders $V_n = \sum_m \eta_m$, meaning that all the phases in the shift operator [Eq. 2] (for every n) are the same.

The long-time behavior of σ and its dependence with α and ζ calls for a more detailed analysis. By analyzing the scaled wavepacket width in the asymptotic limit, $\sigma/N = \sigma(t \to \infty)/N$, versus the scaled correlation length ζ/N, we observe that $\sigma/N \propto (\zeta/N)/[1 + b(\zeta/N)]$ regardless of α, with b being a fit parameter. Therefore for $\zeta/N << 1$ entails that the spreading is proportional to ζ, meaning that if the correlation length is much smaller than the chain size, it dictates the typical localization length. Fig. 4 shows that for a representative case with $\alpha = 1$. For $\zeta > N$ our results indicate that the $\sigma(t \to \infty)/N$ is roughly constant. This unveils that the wavepacket will spread over the entire chain when the typical correlation length becomes much larger than the chain size, the width being proportional to the chain size.

To see it further, in Fig. 5 we plot the scaled wavefunction width versus α for various ζ/N values. It is now seen that the long and short-ranged correlated disorder regimes present quite distinct trends. For $\zeta > N$, we observe that the scaled width of the walker increases monotonically as α is increased. On the other hand, σ/N reaches a maximum around $\alpha \simeq 2$ when $\zeta < N$. This indicates that in the regime of finite correlation lengths (smaller than the chain size), Gaussian-like correlations in the disorder distribution allow for the maximum spreading of the wavepacket, thus signaling the condition of maximum weakening of Anderson localization.

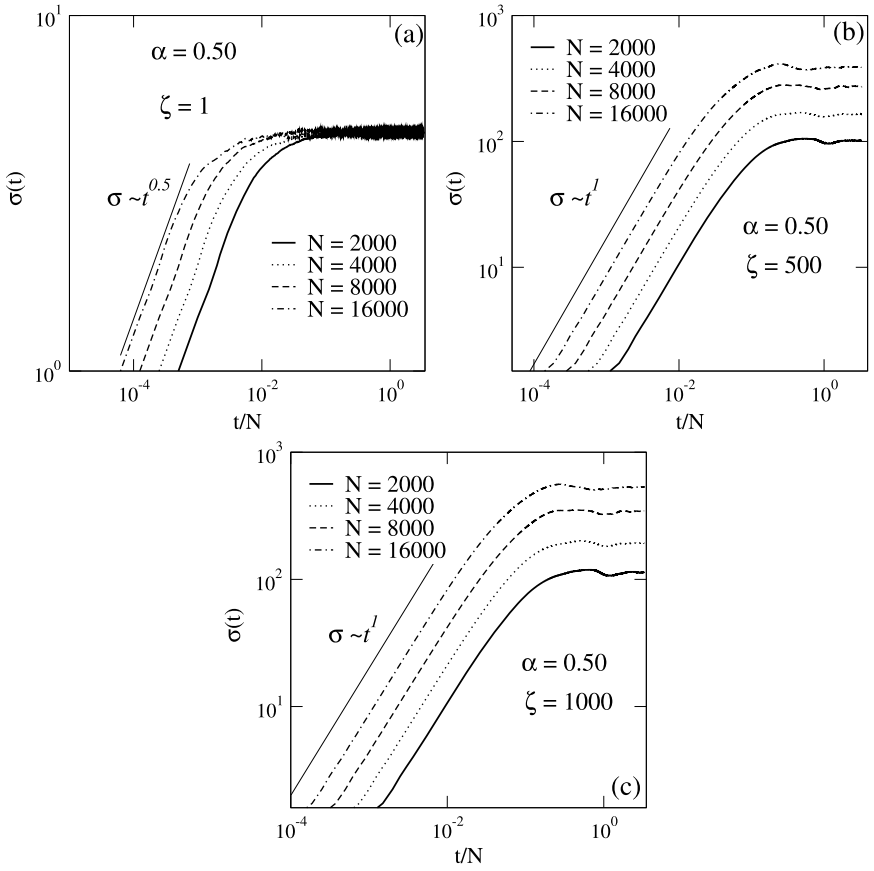

Fig. 3. Standard deviation $\sigma(t)$ versus t/N for (a) $\zeta = 1$, (b) $\zeta = 500$, (c) $\zeta = 1000$, fixed $\alpha = 0.5$, and various system sizes from $N = 2000$ up to 16000.

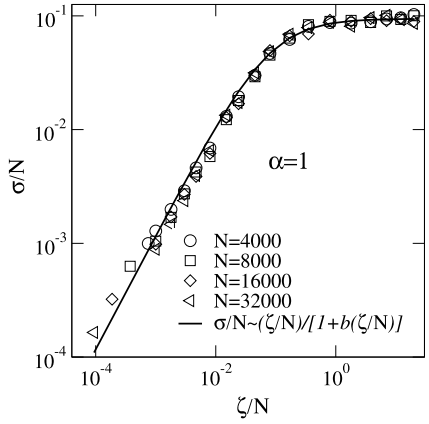

Fig. 4. Scaled long-time wavefunction spreading $\sigma/N = \sigma(t \to \infty)/N$ versus ζ/N for $N = 4000$ up to 32000 and $\alpha = 1$. Solid line is the fitting function, with b being an adjustable parameter.

In order to analyze the ubiquitous behavior around $\alpha = 2$ we carry out a statistical analysis over the disorder distribution by taking series of increments of ϕ_n defined as $\theta_n = \phi_n - \phi_{n-1}$. Therefore, the series $\{\theta_n\}$ contains $N-1$ terms. Next we divide it in s segments of size ζ. The number of segments is then $N_s = N/\zeta$ and we calculate the variance within each segment as $\Delta_s = \sqrt{\langle\theta_n^2\rangle_s - \langle\theta_n\rangle_s^2}$ where $\langle\cdot\rangle_s$ represents the average within segment s. The mean local variance of the increments is finally given by $\Delta = \sum_{s=1}^{N/\zeta} \Delta_s/N_s$. In Fig. 6 we plot Δ (averaged over 20 independent samples) versus α and observe that as it approaches $\alpha = 2$ the local variance decreases suggesting that phase fluctuations are smoother in that region, what explains the trend seen in Fig. 5 for $\zeta < N$.

4. Concluding remarks

In this work we studied the dynamics of a disordered DTQW featuring a generalized exponential correlated phase disorder controlled by two parameters, namely the generalization exponent α and the generalized correlation length ζ. We showed that for $\zeta << N$, the walker remains trapped around its initial position after an initial diffusive spreading, regardless to the α value. Our calculations also indicate that the size of the region over which the walker remains trapped scales as $\sigma \propto \zeta$. On the other hand for $\zeta >> N$ the walker delocalizes ballistically. In this regime increasing α leads to a monotonic increase of the wavepacket width. When the typical correlation length ζ is smaller than the system size N instead, the saturation wavepacket width varies non-monotonically with α, reaching maximum for $\alpha \simeq 2$, slowly decaying for larger values of α. It is worth pointing out that $\alpha = 2$ brings about Gaussian correlations. By evaluating the mean local variance over segments sized by the generalized correlation length, we showed that phase fluctuations get smoother in the vicinity of $\alpha = 2$.

Experiments addressing delocalization transition induced by long-range correlated disorder have put forward ways to manipulate correlations within disordered setups [7]. Efforts along similar lines should bring valuable support for the theoretical predictions concerning discrete-time quantum walk dynamics in distinct disorder regimes.

CRediT authorship contribution statement

C.V.C. Mendes: Conceptualization, Methodology, Numerical calculations of Figs. 3, 4. **G.M.A. Almeida:** Software, Validation, Writing – original draft preparation. **M.L. Lyra:** Software, Validation,

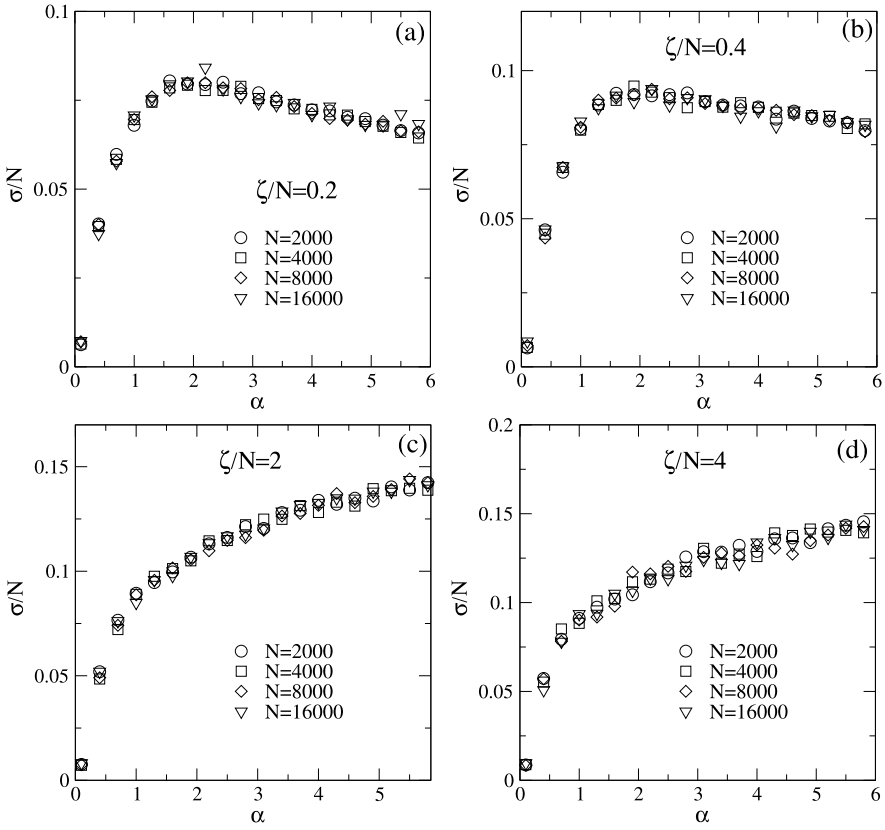

Fig. 5. Scaled long-time wavefunction spreading $\sigma/N = \sigma(t \to \infty)/N$ versus α for (a) $\zeta/N = 0.2$, (b) $\zeta/N = 0.4$, (c) $\zeta/N = 2$, and (d) $\zeta/N = 4$, and $N = 2000$ up to 16000.

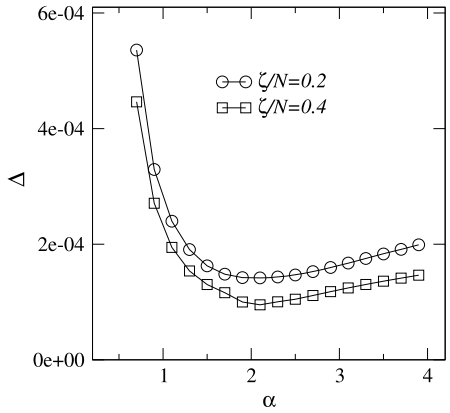

Fig. 6. Mean local variance $\Delta = \sum_{s=1}^{N/\zeta} \Delta_s/N_s$ against α over s segments $\Delta_s = \sqrt{\langle\theta_n^2\rangle_s - \langle\theta_n\rangle_s^2}$, where $\theta_n = \phi_n - \phi_{n-1}$ and $N_s = N/\zeta$. Seen is the result of an average carried out over 20 independent disorder realizations for $\zeta/N = 0.2, 0.4$, with $N = 10000$.

Writing – original draft preparation. **F.A.B.F. de Moura:** Conceptualization, Methodology, Software, Numerical calculations of Figs. 1, 2, 5, 6, Writing – original draft preparation.

Declaration of competing interest

The authors declare that they have no known competing financial interests or personal relationships that could have appeared to influence the work reported in this paper.

Acknowledgements

This work was partially supported by CNPq, CAPES, FINEP, CNPq-Rede Nanobioestruturas, and FAPEAL (Alagoas state agency).

References

[1] F. Evers, A.D. Mirlin, Rev. Mod. Phys. 80 (2008) 1355.
[2] E. Abrahams, P.W. Anderson, D.C. Licciardello, T.V. Ramakrishnan, Phys. Rev. Lett. 42 (1979) 673.
[3] J.C. Flores, J. Phys. Condens. Matter 1 (1989) 8471.
[4] D.H. Dunlap, H.L. Wu, P.W. Phillips, Phys. Rev. Lett. 65 (1990) 88.
[5] F.A.B.F. de Moura, M.L. Lyra, Phys. Rev. Lett. 81 (1998) 3735.
[6] F.M. Izrailev, A.A. Krokhin, Phys. Rev. Lett. 82 (1999) 4062.
[7] U. Kuhl, F.M. Izrailev, A.A. Krokhin, H.-J. Stockmann, Appl. Phys. Lett. 77 (2000) 633.
[8] E. Gurevich, A. Iomin, Phys. Rev. E 83 (2011) 011128.
[9] E. Gurevich, O. Kenneth, Phys. Rev. A 79 (2009) 063617.
[10] G.M. Falco, A.A. Fedorenko, J. Giacomelli, M. Modugno, Phys. Rev. A 82 (2010) 053405.
[11] H. Eleuch, M. Hilke, New J. Phys. 17 (2015) 083061.
[12] F. Izrailev, A. Krokhin, N. Makarov, Phys. Rep. 512 (2012) 125.
[13] S. Sil, S.K. Maiti, A. Chakrabarti, Phys. Rev. B 78 (2008) 113103.
[14] F.A.B.F. de Moura, R.A. Caetano, M.L. Lyra, Phys. Rev. B 81 (2010) 125104.
[15] G.M.A. Almeida, F.A.B.F. de Moura, T.J.G. Apollaro, M.L. Lyra, Phys. Rev. A 96 (2017) 032315.
[16] G.M.A. Almeida, F.A.B.F. de Moura, M.L. Lyra, Phys. Lett. A 382 (2018) 1335.
[17] G.M.A. Almeida, C.V.C. Mendes, M.L. Lyra, F.A.B.F. de Moura, Ann. Phys. 398 (2018) 180.
[18] G.M.A. Almeida, A.M.C. Souza, F.A.B.F. de Moura, M.L. Lyra, Phys. Lett. A 383 (2019) 125847.
[19] Y. Aharonov, L. Davidovich, N. Zagury, Phys. Rev. A 48 (1993) 1687.
[20] J. Kempe, Contemp. Phys. 44 (2003) 307.
[21] N. Shenvi, J. Kempe, K.B. Whaley, Phys. Rev. A 67 (2003) 052307.
[22] N.B. Lovett, S. Cooper, M. Everitt, M. Trevers, V. Kendon, Phys. Rev. A 81 (2010) 042330.
[23] C.M. Chandrashekar, R. Laflamme, Phys. Rev. A 78 (2008) 022314.
[24] H. Obuse, N. Kawakami, Phys. Rev. B 84 (2011) 195139.
[25] T. Kitagawa, M.A. Broome, A. Fedrizzi, M.S. Rudner, E. Berg, I. Kassal, A. Aspuru-Guzik, E. Demler, A.G. White, Nat. Commun. 3 (2012) 882.
[26] E. Flurin, V.V. Ramasesh, S. Hacohen-Gourgy, L.S. Martin, N.Y. Yao, I. Siddiqi, Phys. Rev. X 7 (2017) 031023.
[27] T. Rakovszky, J.K. Asboth, Phys. Rev. A 92 (2015) 052311.
[28] J.M. Edge, J.K. Asboth, Phys. Rev. B 91 (2015) 104202.
[29] A. Wojcik, T. Luczak, P. Kurzynski, A. Grudka, T. Gdala, M. Bednarska-Bzdega, Phys. Rev. A 85 (2012) 012329.

[30] R. Zhang, P. Xue, J. Twamley, Phys. Rev. A 89 (2014) 042317.
[31] F. De Nicola, L. Sansoni, A. Crespi, R. Ramponi, R. Osellame, V. Giovannetti, R. Fazio, P. Mataloni, F. Sciarrino, Phys. Rev. A 89 (2014) 032322.
[32] Q. Zhao, J. Gong, Phys. Rev. B 92 (2015) 214205.
[33] I. Vakulchyk, M.V. Fistul, P. Qin, S. Flach, Phys. Rev. B 96 (2017) 144204.
[34] M. Zeng, E.H. Yong, Sci. Rep. 7 (2017) 12024.
[35] A.R.C. Buarque, W.S. Dias, Phys. Rev. E 100 (2019) 032106.
[36] C.V.C. Mendes, G.M.A. Almeida, M.L. Lyra, F.A.B.F. de Moura, Phys. Rev. E 99 (2019) 022117.
[37] C.-W. Lee, P. Kurzynski, H. Nha, Phys. Rev. A 92 (2015) 052336.
[38] A.R.C. Buarque, W.S. Dias, Phys. Rev. A 101 (2020) 023802.
[39] J.P. Mendonça, F.A.B.F. de Moura, M.L. Lyra, G.M.A. Almeida, Phys. Rev. A 101 (2020) 062335.
[40] A. Schreiber, K.N. Cassemiro, V. Potocek, A. Gabris, I. Jex, C. Silberhorn, Phys. Rev. Lett. 106 (2011) 180403.
[41] A. Crespi, R. Osellame, R. Ramponi, V. Giovannetti, R. Fazio, L. Sansoni, F. De Nicola, F. Sciarrino, P. Mataloni, Nat. Photonics 7 (2013) 322.
[42] J.C. Phillips, Rep. Prog. Phys. 59 (1996) 1133.
[43] J. Kakalios, R.A. Street, W.B. Jackson, Phys. Rev. Lett. 59 (1987) 1037.
[44] D.C. Johnston, Phys. Rev. B 74 (2006) 184430.
[45] M. Kirkengen, J. Bergli, Phys. Rev. B 79 (2009) 075205.
[46] Y.T. Yu, M.Y. Wang, D.W. Zhang, B. Wang, G. Sant, M. Bauchy, Phys. Rev. Lett. 115 (2015) 165901.
[47] W.S. Dias, F.A.B.F. de Moura, M.D. Coutinho-Filho, M.L. Lyra, Phys. Lett. A 374 (2010) 3572.
[48] Y.-K. Yu, P.L. Taylor, E.M. Terentjev, Phys. Rev. Lett. 81 (1998) 128.
[49] O. Flomenbom, et al., Proc. Natl. Acad. Sci. 102 (2005) 2368.
[50] J. Laherrère, D. Sornette, Eur. Phys. J. B 2 (1998) 525.
[51] J.L.L. dos Santos, M.O. Sales, F.A.B.F. de Moura, Physica A 413 (2014) 31.
[52] M.O. Sales, F.A.B.F. de Moura, Physica E 45 (2012) 97.